

## Theoretical Design of Stable Pentacoordinate Boron Compounds

Zhipeng Li, Guoliang Song,\* and Zhen Hua Li\*

Cite This: *ACS Omega* 2022, 7, 2391–2397

Read Online

ACCESS |



Metrics &amp; More

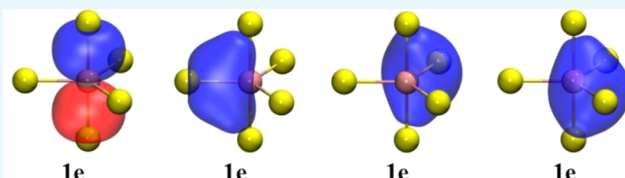


Article Recommendations



Supporting Information

**ABSTRACT:** Through theoretical computations, we found that boron can form thermodynamically stable pentacoordinate compounds. Pentacoordinate boron (penta-B) is just hypercoordinate but not hypervalent because it forms only four covalent bonds, of which at least one is a multicenter bond. Being electron deficient, to be pentacoordinate, at least two of its bonding atoms should have low electronegativity. Penta-B can be formed in  $H_kB(CH_3)_m(XH_3)_n$  ( $X = Si, Ge, Sn$ , and  $n \geq 2$ ) and  $BR_5$  ( $R = BH_2NH_3, AsH_2$ , and  $BeH$ ). Based on a systematic investigation of these model compounds, we designed three thermodynamically stable penta-B compounds that can potentially be synthesized by hydrogenating their tricoordinate counterparts under mild reaction conditions.



$1 \times 3c-2e$  bond    $1 \times 4c-2e$  bond    $1 \times 4c-2e$  bond    $1 \times 4c-2e$  bond  
ON = 1.93 |e|   ON = 1.97 |e|   ON = 1.97 |e|   ON = 1.97 |e|

## INTRODUCTION

Hypercoordination is the property of the main-group elements in a molecule having a larger than normal coordination number, typically greater than four.<sup>1</sup> Hypercoordination is common for the elements in period 3 and beyond.<sup>2</sup> However, it is difficult to form hypercoordinate compounds for the elements in period 2.<sup>3</sup> Over the past few decades, several research studies on hypercoordination in period 2 elements with more than three valence electrons such as carbon and nitrogen have been reported.<sup>2,4</sup> However, for electron-deficient elements such as boron, there is still debate over whether they can form hypercoordinate compounds and what their bonding nature is if they exist.

The attempts on synthesizing hypercoordinate single-boron-center compounds were unsuccessful from our point of view. Since 1984, a series of the so-called pentacoordinate boron (penta-B) compounds has been synthesized, by forcing a tricoordinate boron center to form two additional bonds with Lewis-base ligands.<sup>5,6</sup> However, the two additional B–X ( $X = O, N$ , or  $Cl$ ) bonds in these compounds (B–O:  $\sim 2.4$  Å; B–N:  $\sim 2.5$  Å; and B–Cl:  $\sim 2.7$  Å) are much longer than normal. In addition, Wiberg bond indexes (WBI)<sup>7</sup> of the B–X bonds are all below 0.15. Thus, they can hardly be regarded as real penta-B compounds because there are no covalent bonds formed between B and the other two additional ligands. So far, only one theoretical study mentioned five hypothetical silylboranes whose boron centers look like real pentacoordinate.<sup>8</sup> However, no electronic structure analyses and thermodynamic properties were provided, and it is unknown what their bonding nature is and whether they are thermodynamically stable. Because normal tricoordinate silylboranes can be synthesized and have many interesting properties,<sup>9</sup> we wonder if it is possible to synthesize penta-B compounds from normal tricoordinate silylboranes. Hence, in this work, we first studied the electronic

and geometric properties of a hierarchy of model penta-B compounds to reveal their bonding nature. Then, we try to design several thermodynamically stable silylboranes with a penta-B center that may be synthesized by experiments under mild reaction conditions.

## RESULTS AND DISCUSSION

We first studied the electronic structure and stability of penta-B silylboranes in detail. The geometries of 10 structurally stable silylboranes,  $H_kB(CH_3)_m(SiH_3)_n$  ( $k = 1\sim 5$ ,  $m = 0\sim 2$ ,  $n = 1\sim 5$ , and  $k + m + n = 5$ ), optimized using the M06-2X/aug-cc-pVTZ method,<sup>10</sup> are listed in Figure 1. To be pentacoordinate, the five bonds around B should have normal covalent bond lengths of the ordinary B–H, B–Si, and B–C

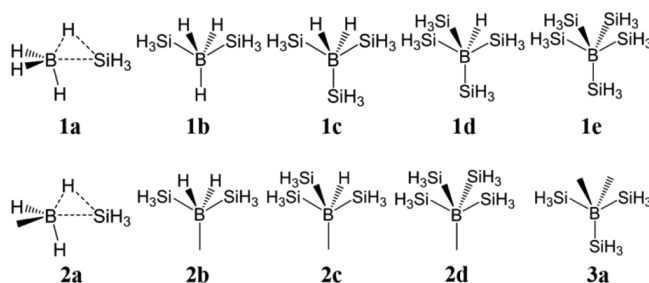
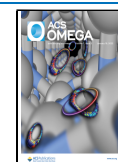


**Figure 1.** Geometries of  $H_kB(CH_3)_m(SiH_3)_n$  ( $k = 1\sim 5$ ,  $m = 0\sim 2$ ,  $n = 1\sim 5$ , and  $k + m + n = 5$ ).

**Received:** November 14, 2021

**Accepted:** December 24, 2021

**Published:** January 4, 2022



bonds, which are about 1.20, 2.03, and 1.56 Å, respectively. The distances of the longest B–Si/B–H bond in each  $H_kB(CH_3)_m(SiH_3)_n$  molecule (results for the B–C bonds are not listed because they all have normal covalent bond lengths) are tabulated in Table 1. The B–Si/B–H bonds in 1b~1e,

**Table 1. Longest B–Si/B–H Bond Lengths in  $H_kB(CH_3)_m(SiH_3)_n$  ( $k = 1\sim 5$ ,  $m = 0\sim 2$ ,  $n = 1\sim 5$ , and  $k + m + n = 5$ )**

	bond length (Å)		bond length (Å)	
1a	2.20/1.30	2a	2.27/1.35	
1b	2.05/1.22	2b	2.09/1.24	
1c	2.02/1.21	2c	2.05/1.23	
1d	2.03/1.21	2d	2.08/–	
1e	2.04/–	3a	2.06/–	

2b~2d, and 3a are all shorter than 2.09/1.24 Å, while in 1a and 2a, they are longer than 2.20/1.30 Å. Therefore, 1b~1e, 2b~2d, and 3a can be regarded as penta-B compounds from a geometrical point of view.

WBI<sup>7</sup> analysis results show that the weakest B–Si/B–H bonds in 1a and 2a are just 0.38/0.62 and 0.33/0.54, respectively. They are certainly neither completely broken nor normal covalent bonds. Both geometrical and WBI data suggest that 1a and 2a are  $\eta^2$ -complexes formed through the interaction between a  $\sigma$  Si–H bond orbital of  $SiH_4$  and the 2p empty orbital of the B center. On the other hand, most of the B–Si/B–H bonds in the other eight molecules can be viewed as weak covalent bonds because their WBIs are in the range of [0.47, 0.84]/[0.77, 0.93] (Table S4). Therefore, they can be regarded as penta-B compounds.

The low WBIs of the B–Si/B–H bonds of the eight molecules suggest that they are not normal single covalent bonds. Meanwhile, the sum of the WBIs of five B–X (X = H, Si, or C) bonds for the eight molecules is no more than 8, implying that no more than four covalent bonds are formed. These results suggest that B must have formed multicenter bonds with its five bonding atoms. Adaptive natural density partitioning (AdNDP) analyses<sup>11</sup> show that there are four, three, and two multicenter bonds around the B center in 1c, 2c, and 3a (Figure 2; Figure S1 for the other five molecules), respectively. These results suggest that boron is not hypervalent,<sup>1</sup> and the Lewis octet rule is not violated. Boron

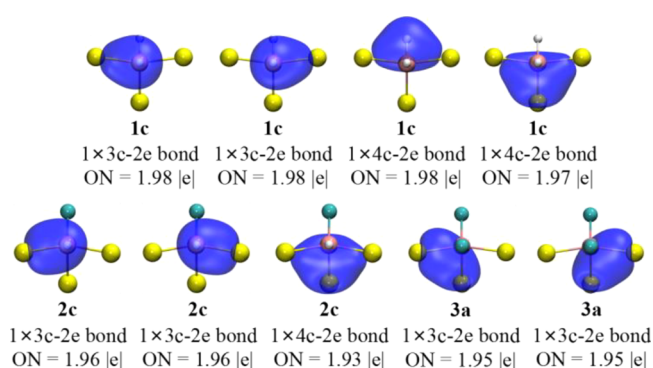


**Figure 2.** AdNDP multicenter orbitals of 1c, 2c, and 3a, where the pink, yellow, cyan, and white balls represent B, Si, C, and H atoms, respectively, and ON is the corresponding occupation number of the AdNDP orbital. H atoms in the silyl and methyl groups are omitted for clarity.

accommodates five bonding atoms by forming multicenter bonds with some of them.

For formation of multicenter bonds, at least two of the bonds between boron and its ligands should not be too strong. It is critical for boron to be hypercoordinate. In addition, because boron is electron deficient, forming covalent bonds requires its bonding atoms to give electrons to boron. Therefore, at least two bonding atoms must have similar electronegativity to boron. Other than silicon, beryllium, germanium, tin, and arsenic also meet such criteria. Replacing the Si atoms by Ge/Sn in  $H_kB(CH_3)_m(SiH_3)_n$  ( $n \geq 2$ ), 16 penta-B compounds (Figure 3) could be optimized. Similarly, 3 penta-B compounds,  $BR_5$  (R =  $BH_2NH_3$ ,  $AsH_2$ , and  $BeH$ ), could be optimized.

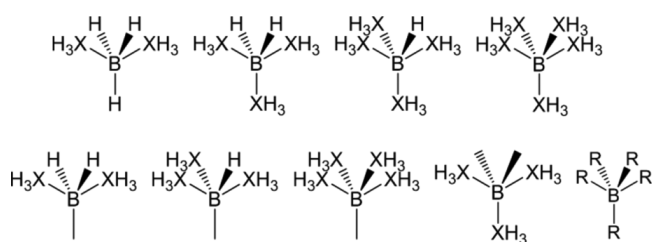


**Figure 3.** Geometries of  $H_kB(CH_3)_m(XH_3)_n$  (X = Ge, Sn,  $k = 1\sim 5$ ,  $m = 0\sim 2$ ,  $n = 2\sim 5$ , and  $k + m + n = 5$ ) and  $BR_5$  (R =  $BH_2NH_3$ ,  $AsH_2$ , and  $BeH$ ).

Hypercoordination usually means instability. Table 2 tabulates the Gibbs free-energy changes ( $\Delta_rG$ ) and barriers

**Table 2. Gibbs Free-Energy Changes ( $\Delta_rG$ ) and Barriers ( $\Delta G^\ddagger$ ) of the Five Decomposition Pathways of 2b at 298.15 K (in kcal/mol) in the Gas Phase<sup>a</sup>**

decomposition products of 2b	$\Delta G^\ddagger$	$\Delta_rG$
$(SiH_3)_2BCH_3 + H_2$	12.0	0.8
$H_2B(SiH_3)CH_3 + SiH_4$	2.9	2.3
$H_2BCH_3 + Si_2H_6$	13.8	–8.6
$HB(SiH_3)_2 + CH_4$	20.3	–0.4
$H_2BSiH_3 + H_3SiCH_3$	23.1	–2.5

<sup>a</sup>The results were computed by the G4//M06-2X/aug-cc-pVTZ method.

( $\Delta G^\ddagger$ ) of five decomposition reactions of 2b (Table S5 for the other seven) at 298.15 K. The results indeed show that these hypothetical compounds are unstable. Among them, releasing  $SiH_4$  is the easiest one with a  $\Delta G^\ddagger$  of just 2.9 kcal/mol. Releasing disilane is the second-easiest one, with a 13.8 kcal/mol  $\Delta G^\ddagger$  and a negative  $\Delta_rG$ . However, the positive  $\Delta_rG$  of the pathway to release  $H_2$  and its low  $\Delta G^\ddagger$  imply that it is possible to synthesize pentacoordinate silylboranes by hydrogenating their tricoordinate counterparts with at least two silyl groups. To obtain pentacoordinate silylboranes stable at room temperature (RT), we need to increase  $\Delta G^\ddagger$  of the lowest-energy decomposition pathway so that they are kinetically stable at RT or increase  $\Delta_rG$  to be positive if  $\Delta G^\ddagger$  must be low so that they are thermochemically stable.

The first attempt we tried is to replace the  $SiH_3$  groups in  $H_kB(CH_3)_m(SiH_3)_n$  by more realistic  $SiR_3$  (R = methyl (Me) or phenyl (Ph)) groups. A total of five such compounds (“A” series) were designed (A1 to A5, Figure S2). Among them, A5 (pentacoordinate  $H_2B(SiPh_3)_3$ ) is a potential candidate of

thermodynamically stable penta-B compounds. To design it, we make use of the  $\pi$ - $\pi$  stack interaction to stabilize **A5** and to increase  $\Delta_r G$  and  $\Delta G^\ddagger$  of the decomposition pathways. In addition to the  $\pi$ - $\pi$  stack effect, another effect could be the electron-withdrawing effect of the phenyl group, which makes Si more electron deficient for forming such hypercoordinate bonding. Table 3 tabulates the  $\Delta G_r$ s and  $\Delta G^\ddagger$ s of three

**Table 3. Gibbs Free-Energy Changes ( $\Delta_r G$ ) and Barriers ( $\Delta G^\ddagger$ ) of Three Possible Decomposition Pathways of **A5** at 298.15 K (in kcal/mol) in Heptane Solution<sup>a</sup>**

decomposition products of <b>A5</b>	$\Delta G^\ddagger$	$\Delta_r G$
$B(\text{SiPh}_3)_3 + \text{H}_2$	31.9	18.3
$\text{HB}(\text{SiPh}_3)_2 + \text{HSiPh}_3$	15.6	12.3
$\text{H}_2\text{BSiPh}_3 + \text{Si}_2\text{Ph}_6$	39.7	9.4

<sup>a</sup>The energies were computed by the M06-2X functional.

possible decomposition pathways of **A5** at 298.15 K in heptane, the solvent to synthesize  $B(\text{SiPh}_3)_3$ .<sup>9a</sup> It should be noted that solvation effect is small for these reactions. The results are indeed promising because all three decomposition pathways have positive  $\Delta_r G$ . Considering that the pathway to  $\text{HB}(\text{SiPh}_3)_2$  has a low  $\Delta G^\ddagger$  and boranes with at least one B-H bond may dimerize, we computed the  $\Delta_r G$  of the reaction  $2\text{A5} \rightarrow (\text{HB}(\text{SiPh}_3)_2)_2 + 2\text{HSiPh}_3$  and  $3\text{H}_2 + 2B(\text{SiPh}_3)_3 \rightarrow 3(\text{SiPh}_3)_2 + \text{B}_2\text{H}_6$ . For the first reaction, we found that it has a positive  $\Delta_r G$  of +1.4 kcal/mol. For the other reaction, although it has a very negative  $\Delta_r G$  of -37.3 kcal/mol, the second step of the reaction, i.e., to release  $\text{Si}_2\text{Ph}_6$  from **A5**, has too high a  $\Delta G^\ddagger$  (39.7 kcal/mol) to occur at RT. These results show that **A5** is indeed thermodynamically stable. In addition, the  $B(\text{SiPh}_3)_3 + \text{H}_2 \rightarrow \text{A5}$  reaction has a negative  $\Delta_r G$  ( $\Delta_r G_{\text{H}_2}$ ) and a moderate  $\Delta G^\ddagger$  ( $\Delta G^\ddagger_{\text{H}_2}$ ) at RT.  $\Delta G^\ddagger_{\text{H}_2}$  is so low that it is possible to synthesize **A5** by hydrogenating  $B(\text{SiPh}_3)_3$  even below RT.

However, a potential disadvantage of synthesizing **A5** is that  $\text{H}_2\text{B}(\text{SiPh}_3)_3$  has two low-energy conformers in fast equilibrium (Figure 4). Except BLYP and B3LYP, other seven

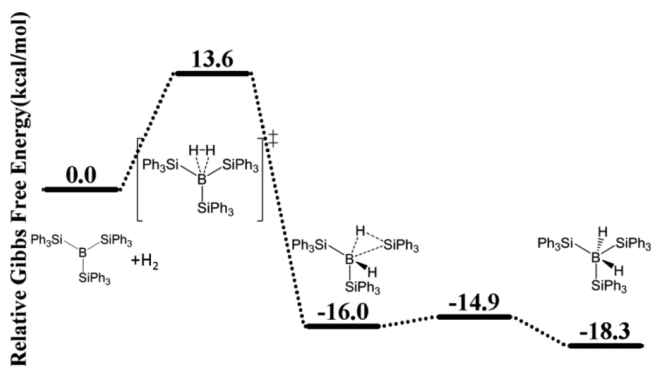


**Figure 4.** Gibbs free-energy profiles of the  $B(\text{SiPh}_3)_3 + \text{H}_2$  reaction at 298.15 K in heptane solution computed by the M06-2X functional.

functionals (PBE,  $\omega$ B97XD, M06-L, MN15-L, M06, M06-2X, and MN15) all give similar results that **A5** is 1.6~3.6 kcal/mol lower in free energy than  $\eta^2\text{-H}_2\text{B}(\text{SiPh}_3)_3$  at 298.15 K (Table S9). Although an  $\sim 2$  kcal/mol free-energy lowering cannot guarantee that the experiment can surely obtain **A5** other than  $\eta^2\text{-H}_2\text{B}(\text{SiPh}_3)_3$  due to uncertainties in theoretical computa-

tions, our results indicate that the chance to observe **A5** by hydrogenating  $B(\text{SiPh}_3)_3$  is high and it is worth a try because  $B(\text{SiPh}_3)_3$  had been synthesized in 1984 with a relatively easy method.<sup>9a</sup>

Other than the “A” series, we have designed other 17 penta-B compounds (Figure S2): the “B” series (**B1** to **B7**) containing two silyl groups, and the “C” series (**C1** to **C7**) containing three silyl groups. Backbones were used to constrain the silyl groups and hinder the release of  $\text{HSiR}_3$  and  $(\text{SiR}_3)_2$ . Their stability and tricoordinate counterparts (removing two bonding H atoms on B) have been studied by searching all possible decomposition and deformation pathways (Figure S3) based on knowledge of chemical bonding and reactions. The  $\Delta_r G$  and  $\Delta G^\ddagger$  values of the lowest-energy pathway are named as  $\Delta_r G_{\text{Min}}$  or  $\Delta G^\ddagger_{\text{Min}}$ , respectively. Promising penta-B candidates should have (1) negative  $\Delta_r G_{\text{H}_2}$  and low  $\Delta G^\ddagger_{\text{H}_2}$ , i.e., they are easy to be synthesized from hydrogenating their tricoordinate counterparts (Table S10), and (2) positive  $\Delta_r G_{\text{Min}}$  or high  $\Delta G^\ddagger_{\text{Min}}$ , i.e. both the pentacoordinate silylborane and its tricoordinate counterpart are stable at RT (Table S11). For  $\Delta G^\ddagger$ , we set the criteria for  $\Delta G^\ddagger_{\text{H}_2}$  to be better below 25 kcal/mol and  $\Delta G^\ddagger_{\text{Min}}$  to be better above 25 kcal/mol, based on an estimation of the half-life of reaction from classical transition state theory. The calculations show that the half-life of a unimolecular reaction is about 66 h and the half-life of a bimolecular reaction is about 94 h at 298.15 K with a  $\Delta G^\ddagger$  of 25 kcal/mol. The geometries of two promising compounds, **B3\_Me** from the “B” series and **C5** from the “C” series that meet such criteria, are presented in Figure 5. Between them, we would recommend the synthesis of **B3\_Me** first because it has fewer backbones and consequently can be synthesized more easily.

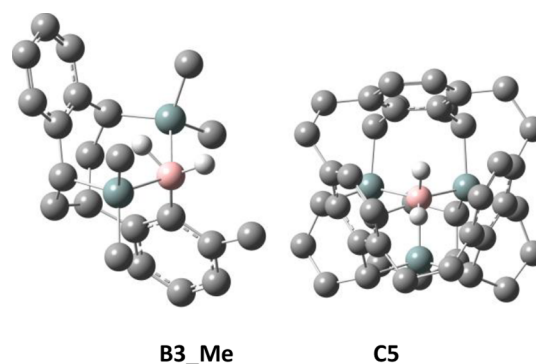


**Figure 5.** Geometries of two stable pentacoordinate silylboranes. Hydrogen atoms on the carbons are omitted for clarity.

Once these pentacoordinate silylboranes are synthesized, they can be verified by NMR spectroscopy. Table 4 tabulates the NPA charges and the  $^{11}\text{B}$  NMR chemical shifts ( $\delta(\text{B})$ ) of simple and recommended silylboranes. Penta-B draws electrons from silyl groups and are negatively charged. Consequently, it is much more shielded than tricoordinate boron and has very negative  $\delta(\text{B})$  values. Indeed, for penta-B silylborane compounds,  $\delta(\text{B})$  has a linear relationship with the NPA charge of the boron atom (Figure S4). On the other hand, neutral tricoordinate silylboranes have very positive  $\delta(\text{B})$  values. In addition,  $\eta^2$ -complex and pentacoordinate conformers can be well differentiated by NMR spectroscopy because  $\delta(\text{B})$  of the pentacoordinate conformer is more

**Table 4.**  $^{11}\text{B}$  NMR Chemical Shifts ( $\delta(\text{B})$ ) and NPA Charges of the B Center in Selected Silylboranes<sup>d</sup>

compound	$\delta(\text{B})$ (ppm)	NPA charge of B (a.u.)
1a	-42.04	-0.54
1b	-57.01	-1.13
1c	-67.37	-1.51
1d	-72.29	-1.72
1e	-78.11	-1.92
2a	-23.65	-0.20
2b	-48.39	-0.75
2c	-60.39	-1.14
2d	-65.33	-1.36
3a	-55.50	-0.84
B(SiPh <sub>3</sub> ) <sub>3</sub>	155.15	-0.18
A5 <sup>a</sup>	-51.92	-1.40
$\eta^2\text{-H}_2\text{B}(\text{SiPh}_3)_3^b$	-37.31	-1.18
B3_Me (-H <sub>2</sub> ) <sup>c</sup>	112.94	0.12
B3_Me	-41.63	-0.87
C5 (-H <sub>2</sub> ) <sup>c</sup>	152.66	-0.39
C5	-56.71	-1.87

<sup>a</sup>Pentacoordinate conformer of  $\text{H}_2\text{B}(\text{SiPh}_3)_3$ , <sup>b</sup> $\eta^2$ -complex conformer of  $\text{H}_2\text{B}(\text{SiPh}_3)_3$ , <sup>c</sup>Tricoordinate counterpart removing two bonding hydrogen atoms on B. <sup>d</sup> $\delta(\text{B})$  was computed by a scaling method at the mPW1PW91/6-311+G(2d,p) level of theory.<sup>12</sup>

negative than that of the  $\eta^2$ -complex conformer: For  $\text{H}_2\text{B}(\text{SiPh}_3)_3$ ,  $\delta(\text{B})$  of A5 is -51.92 ppm, while that of  $\eta^2\text{-H}_2\text{B}(\text{SiPh}_3)_3$  is -37.31 ppm. The same phenomenon can be observed for the hypothetical silylboranes, 1a and 2a. They are two  $\eta^2$ -complexes and their  $\delta(\text{B})$  are just -42.04 and -23.65 ppm, respectively.

## CONCLUSIONS

In summary, boron can be pentacoordinate by forming multicenter covalent bonds with elements, e.g., Be, B, Si, Ge, Sn, and As, having similar electronegativities to boron. We showed that penta-B is not hypervalent and does not violate the Lewis octet rule. Although hypercoordination usually implies instability, we designed three thermodynamically stable pentacoordinate silylboranes, A5, B3\_Me, and C5, that may potentially be synthesized by hydrogenating their tricoordinate counterparts under mild reaction conditions. Potential usage of pentacoordinate silylboranes recommended in this study is hydrogenation catalysts or reductants.

## COMPUTATIONAL METHODS

**Validation of Computational Methods.** First, we took pentacoordinate silylborane  $\text{H}_3\text{B}(\text{SiH}_3)_2$  (Figure 6) as an example to test the effect of basis set and method on the geometry. Eight methods including MP2, M06-2X,<sup>10a</sup>

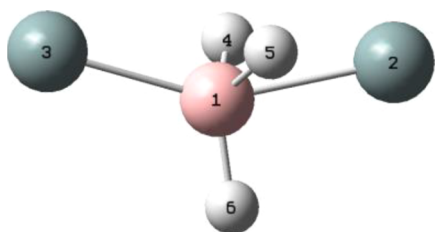


**Figure 6.** Geometry of  $\text{H}_3\text{B}(\text{SiH}_3)_2$  and the indices of atoms. H atoms in the silyl groups are omitted for clarity.

MN15,<sup>13a</sup>  $\omega\text{B97XD}$ ,<sup>13b</sup> PBE0,<sup>13c</sup> TPSSH,<sup>13d</sup> DSD-PBE-P86,<sup>13e,f</sup> and PBE0DH<sup>13g</sup> were tested. Two basis sets were tested: (a) a large basis set in which the aug-cc-pVTZ (AVTZ) basis set<sup>10b-d</sup> was used for all the atoms; (b) a smaller basis set (SBS) in which the 6-31+G(d,p) basis set<sup>14a,b</sup> was used for B and its five bonding atoms, whereas the 6-31G(d,p) basis set<sup>14c-g</sup> was used for the other atoms. Selected bond lengths of  $\text{H}_3\text{B}(\text{SiH}_3)_2$  are listed in Table 5. From the results in Table 5,

**Table 5.** Selected Bond Lengths of  $\text{H}_3\text{B}(\text{SiH}_3)_2$  (Unit: Å)

	B1-Si2	B1-Si3	B1-H4/H5	B1-H6
M06-2X/SBS <sup>a</sup>	2.049	2.007	1.221	1.197
M06-2X/AVTZ <sup>b</sup>	2.037	2.000	1.218	1.197
MN15/SBS	2.038	1.996	1.221	1.198
MN15/AVTZ	2.025	1.984	1.217	1.194
$\omega\text{B97XD}/\text{SBS}$	2.041	2.009	1.224	1.202
$\omega\text{B97XD}/\text{AVTZ}$	2.031	2.001	1.222	1.203
PBE0/SBS	2.029	2.008	1.223	1.202
PBE0/AVTZ	2.024	2.002	1.222	1.203
TPSSH/SBS	2.050	2.016	1.225	1.200
TPSSH/AVTZ	2.040	2.009	1.225	1.203
MP2/SBS	2.049	2.009	1.214	1.192
MP2/AVTZ	2.034	2.004	1.218	1.196
DSDPBEP86/SBS	2.050	2.010	1.222	1.198
DSDPBEP86/AVTZ	2.041	2.005	1.225	1.200
PBE0DH/SBS	2.031	2.002	1.221	1.198
PBE0DH/AVTZ	2.022	1.996	1.222	1.200
standard deviation	0.009	0.007	0.003	0.003
MAD <sup>c</sup>	0.008	0.006	0.002	0.003

<sup>a</sup>SBS: 6-31+G(d,p) for B and its five bonding atoms and 6-31G(d,p) for other atoms. <sup>b</sup>AVTZ: aug-cc-pVTZ. <sup>c</sup>Mean absolute deviation between the two basis sets for the eight methods.

it can be concluded that the method and basis set both have small effect on the geometry of  $\text{H}_3\text{B}(\text{SiH}_3)_2$ : The standard deviation of all 16 combinations of methods and basis sets is below 0.01 Å for each B-X (X = H or Si) bond; the mean absolute deviation between the two basis sets for the eight methods is also below 0.01 Å for each B-X bond.

Second, we tested the performance of density functional theory (DFT) methods on computing relative energies. We used the M06-2X/AVTZ method to optimize the geometries of eight pent-B silylboranes,  $\text{H}_k\text{B}(\text{CH}_3)_m(\text{SiH}_3)_n$  ( $k = 1\sim 5$ ,  $m = 0\sim 2$ ,  $n = 2\sim 5$ , and  $k + m + n = 5$ ). A total of 23 decomposition reactions (Table S2) for them were studied. The geometry optimizations and harmonic vibrational frequency analyses of the reactants, transition states, and products were all performed with the M06-2X/AVTZ method. The G4 method<sup>15</sup> was used to perform single-point energy calculations on these optimized geometries. The errors of the M06-2X method using two basis sets, AVTZ and SBS, on the energetics of the 23 reactions are summarized in Table 6. The results in Table 6 indicate that the smaller basis set (SBS) systematically underestimates the reaction energies and energy barriers by about 1 kcal/mol. On the other hand, using a larger basis set, AVTZ, there is almost no systematic error because the mean error is close to 0. In addition, using AVTZ, both reaction energies and energy barriers are improved and the overall root mean square error (RMSE) over 46 relative energies is just 1.2 kcal/mol. Therefore, these results indicate that geometry optimization can be performed using an SBS, whereas a larger basis set is better to be used to further refine the energetic

**Table 6. Mean Error (ME), Mean Unsigned Error (MUE), and Root Mean Square Error (RMSE) of the M06-2X Method Using the AVTZ and SBS Basis Sets on Computing All 46 Relative Energies of the Reaction Using G4 as the Standard (Unit: kcal/mol)**

	total <sup>a</sup>	
	M06-2X/SBS <sup>b</sup>	M06-2X/AVTZ <sup>c</sup>
ME	-1.1	0.0
MUE	1.2	1.0
RMSE	1.6	1.2

<sup>a</sup>The G4 results were computed at the G4//M06-2X/AVTZ level.

<sup>b</sup>SBS: 6-31+G(d,p) for B and its five bonding atoms and 6-31G(d,p) for other atoms. Geometries were fully optimized using this basis set.

<sup>c</sup>AVTZ: aug-cc-pVTZ. Geometries were fully optimized using this basis set.

results. In the present study, for small systems, we used the M06-2X/AVTZ method to optimize geometry and used the G4 method to perform single-point energy calculations. For large systems where G4 calculations are prohibitively expensive, we used M06-2X/SBS to optimize geometry and a larger basis set to perform single-point energy calculations. The basis set used for single-point energy calculations is also a combined basis set: the AVTZ basis set was used for B and its five bonding atoms, and the aug-cc-pVDZ (AVDZ) basis set was used for the other atoms. This combination basis set was abbreviated as LBS. LBS is a compromise between accuracy and efficiency because for those key atoms involved in bond making and broken processes, the large AVTZ basis set was used, whereas for other “observing” atoms, a smaller AVDZ basis set was used.

Although G4 is very accurate, it is prohibitively expensive for large systems. We should find a cheaper method as accurate as possible. In the present study, we tested a total of 11 DFT functional methods: two GGA functionals, BLYP and PBE; two hybrid GGA functionals, B3LYP and  $\omega$ B97XD; two meta-GGA functionals, M06-L and MN15-L; three hybrid meta-GGA functionals, M06, M06-2X, and MN15; and two double hybrid GGA functionals, PBE0DH and DSD-PBEP86. All energetic results were obtained by performing single-point energy calculations on geometries optimized with the M06-2X/AVTZ method. The errors of these functionals using G4 as the standard are summarized in Table 7. The results in Table 7 indicate that M06-2X is the best method, which has the smallest error on both reaction energy changes and energy barriers. Therefore, for the calculations of large systems, we will use the M06-2X/SBS method to perform both geometry optimizations and vibrational frequency analyses. Then, we will use the M06-2X/LBS method to perform single-point energy calculations.

**Table 7. Mean Error (ME), Mean Unsigned Error (MUE), and Root Mean Square Error (RMSE) of All 46 Relative Energies of 11 DFT Methods Using G4 as the Standard (Unit: kcal/mol)<sup>a</sup>**

	BLYP	PBE	B3LYP	$\omega$ B97XD	M06-L	MN15-L	M06	M06-2X	MN15	PBE0DH	DSD-PBEP86
ME	-8.2	1.1	-6.9	-1.9	0.8	0.5	-0.8	0.0	2.1	-1.5	-8.0
MUE	8.3	2.5	7.0	2.1	2.4	1.3	1.9	1.0	2.3	2.2	8.3
RMSE	10.5	3.0	9.1	2.8	3.2	1.6	2.2	1.2	3.0	3.3	9.7

<sup>a</sup>All 46 relative energies: 23 potential energy changes and 23 potential energy barriers of the reaction. Single-point energy calculations were performed on geometries optimized with the M06-2X/AVTZ method.

**Computational Details.** All quantum calculations were performed with the Gaussian 16 program package.<sup>16</sup> Wiberg bond indices,<sup>7</sup> NPA atomic charges, and AdNDP orbitals<sup>11</sup> were performed with the NBO<sup>17</sup> and Multiwfn programs.<sup>18</sup> In all the DFT calculation, a pruned (99,590) grid (using keyword “int. = ultrafine” in Gaussian 16) was used. Solvation effect was considered using the polarizable continuum solvation model<sup>19a</sup> with radii and nonelectrostatic terms for Truhlar and co-workers’ SMD solvation model.<sup>19b</sup> Except H<sub>2</sub>, for which it is a gas under standard state, Gibbs free energy of a compound in the solution ( $G_T$ ) is computed by the following equation:

$$G_T = E_e + \text{ZPE} + \Delta G_{0 \rightarrow T} + 1.9 \text{ kcal/mol},$$

where  $E_e$  is the electronic energy computed with solvation effect considered, ZPE and  $\Delta G_{0 \rightarrow T}$  are the zero-point vibrational correction and thermal correction to Gibbs free energy in the gas phase computed by the M06-2X/SBS method, and 1.9 kcal/mol is the correction from the gas-phase standard state of 1 bar to the solution standard state of 1 mol/L. The geometry used for the single-point calculation in the solution was optimized in the gas phase.

<sup>11</sup>B NMR chemical shifts were computed by a well validated method.<sup>12</sup> In this method, NMR calculations were computed with the mPW1PW91/6-311+G(2d,p) method in THF solution under the SMD solvation model. The <sup>11</sup>B NMR chemical shift ( $\delta(B)$ , in ppm) was computed using the following scaling equation:

$$\delta(B) = \frac{\text{intercept} - \sigma}{-\text{slope}}$$

where  $\sigma$  is the computed isotropic shielding constant, and the intercept and slope are 106.67 ppm and -1.1050, respectively.

## ■ ASSOCIATED CONTENT

### Supporting Information

The Supporting Information is available free of charge at <https://pubs.acs.org/doi/10.1021/acsomega.1c06415>.

Validation of computational methods, computational details, other supplementary materials, and Cartesian coordinates of recommended pentacoordinate boron compounds (PDF)

## ■ AUTHOR INFORMATION

### Corresponding Authors

Guoliang Song – Shanghai Key Laboratory of Molecular Catalysis and Innovative Material, Department of Chemistry, Fudan University, Shanghai 200438, China; [orcid.org/0000-0003-0445-5996](https://orcid.org/0000-0003-0445-5996); Email: [guoliangsong@fudan.edu.cn](mailto:guoliangsong@fudan.edu.cn)

Zhen Hua Li – Shanghai Key Laboratory of Molecular Catalysis and Innovative Material, Department of Chemistry, Fudan University, Shanghai 200438, China; [orcid.org/0000-0002-5636-9865](https://orcid.org/0000-0002-5636-9865); Email: [lizhenhua@fudan.edu.cn](mailto:lizhenhua@fudan.edu.cn)

## Author

Zhipeng Li – Shanghai Key Laboratory of Molecular Catalysis and Innovative Material, Department of Chemistry, Fudan University, Shanghai 200438, China

Complete contact information is available at:

<https://pubs.acs.org/10.1021/acsomega.1c06415>

## Notes

The authors declare no competing financial interest.

## ACKNOWLEDGMENTS

Financial support from the National Natural Science Foundation of China (NSCF) (21873019 and 22173021) is gratefully acknowledged.

## REFERENCES

- (1) IUPAC. *Compendium of Chemical Terminology*, 2nd ed. (the "Gold Book"). Compiled by McNaught, A. D.; Wilkinson, A.; Blackwell Scientific Publications: Oxford, 1997. Online version (2019-) created by Chalk, S. J.
- (2) For silicon: (a) Brook, M. A. In *Silicon in Organic, Organometallic and Polymer Chemistry*; Wiley: New York, 2000. (b) Kost, D.; Kalikhman, I. Hypercoordinate Silicon Complexes Based on Hydrazide Ligands. A Remarkably Flexible Molecular System. *Acc. Chem. Res.* **2009**, *42*, 303–314. For phosphorus: (c) Holmes, R. R. *Pentacoordinated Phosphorus*, ACS Monographs 175 and 176; American Chemical Society: Washington, DC, 1980; Vol. 1 and 2. For sulfur: (d) Martin, J. C. "Frozen" Transition States: Pentavalent Carbon et al. *Science* **1983**, *221*, 509–514.
- (3) (a) Reed, A. E.; Schleyer, P. V. R. Chemical Bonding in Hypervalent Molecules. The Dominance of Ionic Bonding and Negative Hyperconjugation over d-orbital Participation. *J. Am. Chem. Soc.* **1990**, *112*, 1434–1445. (b) Magnusson, E. Hypercoordinate Molecules of Second-row Elements: d Functions or d Orbitals? *J. Am. Chem. Soc.* **1990**, *112*, 7940–7951.
- (4) (a) Forbus, T. R., Jr.; Martin, J. C. Quest for an Observable Model for the  $\text{SN}_2$  Transition State. Pentavalent Pentacoordinate Carbon. *J. Am. Chem. Soc.* **1979**, *101*, 5057–5059. (b) Ewig, C. S.; Van Wazer, J. R. Ab Initio Studies of Molecular Structures and Energetics. 3. Pentacoordinated Nitrogen  $\text{NF}_n\text{H}_{5-n}$  Compounds. *J. Am. Chem. Soc.* **1989**, *111*, 4172–4178. (c) Michels, H. H.; Montgomery, J. A., Jr. The Electronic Structure and Stability of  $\text{NF}_5$  and  $\text{PF}_5$ . *J. Chem. Phys.* **1990**, *93*, 1805–1813. (d) Bettinger, H. F.; Schleyer, P. V. R.; Schaefer, H. F. III.  $\text{NF}_5$  – Viable or Not? *J. Am. Chem. Soc.* **1998**, *120*, 11439–11448. (e) Ponec, R.; Roithová, J. Domain-Averaged Fermi Holes – A New Means of Visualization of Chemical Bonds. Bonding in Hypervalent Molecules. *Theor. Chem. Acc.* **2001**, *105*, 383–392.
- (5) Lee, D. Y.; Martin, J. C. Compounds of Pentacoordinate (10-B-5) and Hexacoordinate (12-B-6) Hypervalent Boron. *J. Am. Chem. Soc.* **1984**, *106*, 5745–5746.
- (6) (a) Yamashita, M.; Yamamoto, Y.; Akiba, K.; Nagase, S. Synthesis of A Versatile Tridentate Anthracene Ligand and Its Application for the Synthesis of Hypervalent Pentacoordinate Boron Compounds (10-B-5). *Angew. Chem.* **2000**, *112*, 4221–4224. (b) Yamashita, M.; Yamamoto, Y.; Akiba, K.; Hashizume, D.; Iwasaka, F.; Takagi, N.; Nagase, S. Syntheses and Structures of Hypervalent Pentacoordinate Carbon and Boron Compounds Bearing an Anthracene Skeleton – Elucidation of Hypervalent Interaction Based on X-ray Analysis and DFT Calculation. *J. Am. Chem. Soc.* **2005**, *127*, 4354–4371. (c) Nakatsuji, J.-Y.; Moriyama, Y.; Matsukawa, S.; Yamamoto, Y.; Akiba, K. Synthesis and Structure of Hypervalent Boron (10-B-5) Compounds Bearing a 2,6-(p-tolyloxymethyl)benzene Tridentate Ligand. *Main Group Chem.* **2006**, *5*, 277–285. (d) Hirano, Y.; Kojima, S.; Yamamoto, Y. A Hypervalent Pentacoordinate Boron Compound with an N-B-N Three-Center Four-electron Bond. *J. Org. Chem.* **2011**, *76*, 2123–2131. (e) Dou, C.; Saito, S.; Yamaguchi, S. A Pentacoordinate Boron-Containing  $\pi$ -Electron System with Cl-B-Cl Three-Center Four-Electron Bonds. *J. Am. Chem. Soc.* **2013**, *135*, 9346–9349. (f) McGovern, G. P.; Zhu, D.; Aquino, A. J. A.; Vidović, D.; Findlater, M. Synthesis and Characterization of Terpyridine-Supported Boron Cations: Evidence for Pentacoordination at Boron. *Inorg. Chem.* **2013**, *52*, 13865–13868.
- (7) Wiberg, K. B. Application of the Pople-Santry-Segal CNDO Method to the Cyclopropylcarbonyl and Cyclobutyl Cation and to Bicyclobutane. *Tetrahedron* **1968**, *24*, 1083–1096.
- (8) Konczol, L.; Turczel, G.; Szpisjak, T.; Szieberth, D. The Stability of  $\eta^2\text{-H}_2$  Borane Complexes – A Theoretical Investigation. *Dalton Trans.* **2014**, *43*, 13571–13577.
- (9) (a) Pachaly, B.; West, R. Photochemical Generation of Triphenylsilylboranediyl ( $\text{C}_6\text{H}_5$ )<sub>3</sub>SiB: From Organosilylboranes. *Angew. Chem., Int. Ed. Engl.* **1984**, *23*, 454–455. (b) Suginome, M.; Ito, Y. Transition-Metal-Catalyzed Additions of Silicon-Silicon and Silicon-Heteroatom Bonds to Unsaturated Organic Molecules. *Chem. Rev.* **2000**, *100*, 3221–3256. (c) Oestreich, M.; Hartmann, E.; Mewald, M. Activation of the Si-B Interelement Bond: Mechanism, Catalysis, and Synthesis. *Chem. Rev.* **2013**, *113*, 402–441. (d) Wang, H.; Wu, L. L.; Lin, Z. Y.; Xie, Z. W. Transition-Metal-Like Behavior of Monovalent Boron Compounds: Reduction, Migration, and Complete Cleavage of CO at a Boron Center. *Angew. Chem., Int. Ed.* **2018**, *57*, 8708–8713.
- (10) (a) Zhao, Y.; Truhlar, D. G. The M06 Suite of Density Functionals for Main Group Thermochemistry, Thermochemical Kinetics, Noncovalent Interactions, Excited States, and Transition Elements: Two New Functionals and Systematic Testing of Four M06-Class Functionals and 12 Other Functionals. *Theor. Chem. Acc.* **2008**, *120*, 215–241. (b) Dunning, T. H. Gaussian Basis Sets for Use in Correlated Molecular Calculations. I. The Atoms Boron Through Neon and Hydrogen. *J. Chem. Phys.* **1989**, *90*, 1007–1023. (c) Kendall, R. A.; Dunning, T. H.; Harrison, R. J. Electron Affinities of the First-Row Atoms Revisited. Systematic Basis Sets and Wave Functions. *J. Chem. Phys.* **1992**, *96*, 6796–6806. (d) Woon, D. E.; Dunning, T. H. Gaussian Basis Sets for Use in Correlated Molecular Calculations. III. The Atoms Aluminum through Argon. *J. Chem. Phys.* **1993**, *98*, 1358–1371.
- (11) Zubareva, D. Y.; Boldyrev, A. I. Developing Paradigms of Chemical Bonding: Adaptive Natural Density Partitioning. *Phys. Chem. Chem. Phys.* **2008**, *10*, 5207–5217.
- (12) Gao, P.; Wang, X.; Huang, Z.; Yu, H. <sup>11</sup>B NMR Chemical Shift Predictions via Density Functional Theory and Gauge-Including Atomic Orbital Approach: Applications to Structural Elucidations of Boron-Containing Molecules. *ACS Omega* **2019**, *4*, 12385–12392.
- (13) (a) Yu, H. S.; He, X.; Li, S. L.; Truhlar, D. G. MN15: A Kohn–Sham global-hybrid exchange–correlation density functional with broad accuracy for multi-reference and single-reference systems and noncovalent interactions. *Chem. Sci.* **2016**, *7*, 5032–5051. (b) Chai, J. D.; Head-Gordon, M. Long-range corrected hybrid density functionals with damped atom–atom dispersion corrections. *Phys. Chem. Chem. Phys.* **2008**, *10*, 6615–6620. (c) Adamo, C.; Barone, V. Toward reliable density functional methods without adjustable parameters: The PBE0 model. *J. Chem. Phys.* **1999**, *110*, 6158–6170. (d) Tao, J. M.; Perdew, J. P.; Staroverov, V. N.; Scuseria, G. E. Climbing the Density Functional Ladder: Nonempirical Meta-Generalized Gradient Approximation Designed for Molecules and Solids. *Phys. Rev. Lett.* **2003**, *91*, No. 146401. (e) Kozuch, S.; Martin, J. M. L. DSD-PBEP86: in search of the best double-hybrid DFT with spin-component scaled MP2 and dispersion corrections. *Phys. Chem. Chem. Phys.* **2011**, *13*, 20104–20107. (f) Kozuch, S.; Martin, J. M. L. Spin-component-scaled double hybrids: An extensive search for the best fifth-rung functionals blending DFT and perturbation theory. *J.*

*Comput. Chem.* **2013**, *34*, 2327–2344. (g) Brémond, É.; Adamo, C. Seeking for parameter-free double-hybrid functionals: The PBE0-DH model. *J. Chem. Phys.* **2011**, *135*, No. 024106.

(14) (a) Clark, T.; Chandrasekhar, J.; Spitznagel, G. W.; Schleyer, P. V. R. Efficient diffuse function-augmented basis sets for anion calculations. III.† The 3-21+G basis set for first-row elements, Li–F. *J. Comput. Chem.* **1983**, *4*, 294–301. (b) Dill, J. D.; Pople, J. A. Self-consistent molecular orbital methods. XV. Extended Gaussian-type basis sets for lithium, beryllium, and boron. *J. Chem. Phys.* **1975**, *62*, 2921–2923. (c) Ditchfield, R.; Hehre, W. J.; Pople, J. A. Self-Consistent Molecular-Orbital Methods. IX. An Extended Gaussian-Type Basis for Molecular-Orbital Studies of Organic Molecules. *J. Chem. Phys.* **1971**, *54*, 724–728. (d) Francl, M. M.; Pietro, W. J.; Hehre, W. J.; Binkley, J. S.; Gordon, M. S.; DeFrees, D. J.; Pople, J. A. Self-consistent molecular orbital methods. XXIII. A polarization-type basis set for second-row elements. *J. Chem. Phys.* **1982**, *77*, 3654–3665. (e) Gordon, M. S.; Binkley, J. S.; Pople, J. A.; Pietro, W. J.; Hehre, W. J. Self-consistent molecular-orbital methods. 22. Small split-valence basis sets for second-row elements. *J. Am. Chem. Soc.* **1982**, *104*, 2797–2803. (f) Hariharan, P. C.; Pople, J. A. The influence of polarization functions on molecular orbital hydrogenation energies. *Theor. Chim. Acta* **1973**, *28*, 213–222. (g) Hehre, W. J.; Ditchfield, R.; Pople, J. A. Self-Consistent Molecular Orbital Methods. XII. Further Extensions of Gaussian-Type Basis Sets for Use in Molecular Orbital Studies of Organic Molecules. *J. Chem. Phys.* **1972**, *56*, 2257–2261.

(15) Curtiss, L. A.; Redfern, P. C.; Raghavachari, K. Gaussian-4 theory. *J. Chem. Phys.* **2007**, *126*, No. 084108.

(16) Frisch, M. J.; Trucks, G. W.; Schlegel, H. B.; Scuseria, G. E.; Robb, M. A.; Cheeseman, J. R.; Scalmani, G.; Barone, V.; Petersson, G. A.; Nakatsuji, H.; et al. *Gaussian 16, Revision B.01*; Gaussian, Inc.: Wallingford, CT, 2016.

(17) (a) Foster, J. P.; Weinhold, F. Natural hybrid orbitals. *J. Am. Chem. Soc.* **1980**, *102*, 7211–7218. (b) Reed, A. E.; Weinhold, F. Natural localized molecular orbitals. *J. Chem. Phys.* **1985**, *83*, 1736–1740. (c) Reed, A. E.; Weinstock, R. B.; Weinhold, F. Natural population analysis. *J. Chem. Phys.* **1985**, *83*, 735–746. (d) Reed, A. E.; Curtiss, L. A.; Weinhold, F. Intermolecular interactions from a natural bond orbital, donor-acceptor viewpoint. *Chem. Rev.* **1988**, *88*, 899–926.

(18) Lu, T.; Chen, F. W. Multiwfn: A multifunctional wavefunction analyzer. *J. Comput. Chem.* **2012**, *33*, 580–592.

(19) (a) Scalmani, G.; Frisch, M. J.; Map, V. Continuous surface charge polarizable continuum models of solvation. I. General formalism. *J. Chem. Phys.* **2010**, *132*, 114110. (b) Marenich, A. V.; Cramer, C. J.; Truhlar, D. G. Universal Solvation Model Based on Solute Electron Density and on a Continuum Model of the Solvent Defined by the Bulk Dielectric Constant and Atomic Surface Tensions. *J. Phys. Chem. B* **2009**, *113*, 6378–6396.